Math. Model. Nat. Phenom.
Vol. 11, No. 3, 2016, pp. 142–156
DOI: 10.1051/mmnp/20161139

A Mathematical Model for the Proliferation, Accumulation and Spread of Pathogenic Proteins Along Neuronal Pathways with Locally Anomalous Trapping

C. N. Angstmann[1], I. C. Donnelly[1], B. I. Henry[1] *, T. A. M. Langlands[2]
[1] School of Mathematics and Statistics
UNSW Australia
[2] School of Agricultural, Computational and Environmental Sciences
University of Southern Queensland, Australia

Abstract. There is growing evidence that many neurodegenerative disease processes involve the proliferation, accumulation and spread of pathogenic proteins. The transport of proteins in the brain is typically hindered on small scales by micro-domain traps and binding sites but it may be enhanced on larger scales by neuronal pathways identified as white matter transport networks. We have introduced a mathematical network model to simulate a pathogenic protein neurodegenerative disease in the brain taking into account the anomalous transport. The proliferation and accumulation of pathogenic proteins is modelled using a set of reaction kinetics equations on the nodes of a network. Transport of the proteins on the network is modelled as a continuous time random walk with power law distributed waiting times on the nodes. This power law waiting time distribution is shown to be consistent with anomalously slowed diffusion on local scales but transport is enhanced on larger scales by the jumps between nodes. The model reveals that the disease spreads as a propagating front throughout the brain. The anomalous behaviour leads to a lessor variation in the concentration of pathogenic proteins. The enhanced transport on the network ensures that the approach to equilibrium is dominated by the short time behaviour of the waiting time density, hence the effects of subdiffusion are not as pronounced as in a spatial continuum.

Keywords and phrases: anomalous transport, fractional diffusion, prion disease

Mathematics Subject Classification: 34A08, 37H10, 60G20, 92B05, 90B15, 92C20

1. Introduction

Many neurodegenerative disease processes are thought to involve pathogenic misfolded proteins that cause other proteins to misfold and aggregate together disrupting the normal functioning of nerve cells [1]. These misfolded proteins are hypothesised to spread along neuronal pathways to other regions of the brain seeding further misfolding and aggregation there. The canonical example [2] involves proteinaceous

*Corresponding author. E-mail: b.henry@unsw.edu.au

infectious particles, known as prions, implicated in diseases such as Creutzfeldt-Jakob disease, Gerstmann-Sträussler-Scheinker disease, kuru, fatal insomnia, bovine spongiform encephalopathy, scrapie and chronic wasting disease [1,3,4]. The mammalian prion protein, PrP, is the only known prion in mammals, however there are other proteins that are "prion-like". These proteins are known as prionoids [5] and examples include, amyloid-β and tau [6], which are involved with Alzheimer's disease [7], and α-synuclein, which is involved with Parkinson's disease [8, 9]. Whilst prions and prionoids are very similar [6, 10] there is evidence both for [11, 12] and against [13] the hypothesis that they are the same.

The mechanics of prion diseases involves the normal cellular protein PrP^C and the pathogenic form of the same protein PrP^{Sc} [3]. It has been observed that PrP^{Sc} form catalyses PrP^C to misfold and transform into PrP^{Sc}. Also the PrP^{Sc} will form aggregates. In the presence of PrP^{Sc}, the continuous production of PrP^C from neurons results in the accumulation of these aggregates and the disruption of proper neural functioning [3]. A similar chain of events is thought to happen to prionoids [6, 10].

For each of the prion and prionoid diseases, characteristic effects are observed at a macroscopic level. These are manifest as spongiform degeneration and aggregates of PrP^{Sc} in prion diseases [14], aggregates of Amyloid-β aggregates in Alzheimer's disease [7] and α-synuclein containing Lewy bodies in Parkinson's disease [8]. Understanding the aggregation and the spread of the aggregates is a major open problem [1, 10, 15].

The exact mechanism of prion transport in the brain is unknown but it is thought to occur across the white matter neural pathways [16–22]. Transport along these pathways can be identified as a transport network [23] obtained from Diffusion Tensor Imaging (DTI) [24]. DTI provides a mapping of the diffusion of water molecules in the brain. Previous work has shown links between the structure of the white matter transport network and the spread of Alzheimer's disease [25].

The diffusion of molecules in the extracellular space are hindered by micro-domain traps, binding sites, and obstruction from other molecules in the extracellular matrix space [26]. Collectively such barriers may result in anomalously slowed diffusion [27,28] that has been characterised variously through; reduced apparent diffusion constants [29, 30], biexponential behaviour [31], stretched exponential behaviour [32–35], kurtosis [36], and fractional subdiffusion [33, 37, 38]. Extracellular transport of proteins in the brain may be further complicated by their uptake and release from cells [39, 40].

One of the most well studied and commonly observed manifestations of anomalously slowed diffusion is fractional subdiffusion [41, 42]. Here the mean square displacement grows as a sub linear power law in time, characterised by an anomalous exponent α. Fractional subdiffusion can be derived from a continuous time random walk (CTRW) model in which particles wait for a random time, given by a power law or Mittag-Leffler waiting time density, before jumping to a new location [41]. In a spatial continuum the limit process of CTRWs can be formulated as fractional diffusion equations [41, 42], fractional Fokker-Planck equations [43–45], and fractional reaction-diffusion equations [46–48]. In subdiffusion with reactions on a spatial continuum propagating fronts have been analyzed [47, 49, 50]. Further extensions to include the effects of an electric field have been used to formulate a fractional cable equation [51–53] as a mathematical model for the electronic properties of dendrites, taking into account trapping by dendritic spines. On a larger scale, the fractional diffusion equation has been used to calibrate anomalous diffusion in MRI images of the brain [54]. The CTRW model has also been extended to networks, including the effects of reactions [55] and forces [56].

In this paper we have introduced a mathematical network model to describe a pathogenic protein neurodegenerative disease in the brain taking into account transport along neural pathways and locally anomalous diffusion. The proliferation and accumulation of pathogenic proteins is modelled using reaction kinetics on the nodes of a white matter transport network. The spread of the disease is modelled using a CTRW on the network with power law distributed waiting times at the nodes [55]. The power law distributed waiting times model the locally anomalous subdiffusion. As a particular application we consider a simple hetrodimer model of PrP [57] on the white matter transport network with local subdiffusion. The model includes the reaction kinetics of PrP^{Sc} causing PrP^C to misfold then aggregate. The governing generalised master equations for the disease process are solved numerically using an implicit

time-stepping method [58]. Numerical simulations have been carried out for two anomalous exponents, $\alpha = 0.6$ and $\alpha = 0.8$, and for locally standard diffusion where $\alpha = 1$. The values of the anomalous exponents considered are consistent with reported values [33, 35, 54].

2. A Network Mathematical Model for Prion Dynamics

Our mathematical model for prion dynamics considers three agents, normal cellular proteins PrP^C, pathogenic proteins, PrP^{Sc}, and stationary aggregates of pathogenic proteins, PrP^{Agg}, and is based on the hetrodimer model [57]. The model is composed of a set of coupled ordinary differential equations (ODEs) to describe the temporal evolution of the concentration of each of the proteins. The model reaction kinetics consist of: production of PrP^C by cells, degradation of PrP^C, catalysis of PrP^C into PrP^{Sc}, degradation of PrP^{Sc} and aggregation of PrP^{Sc}. We assume the prions move on a white matter transport network consisting of N nodes, $\{v_1, ..., v_N\}$. The aggregates, which accumulate at the nodes, are assumed to be stationary. The model assumes three basic features: (i) Reactions occur on the nodes of a network. (ii) Transport occurs as transitions between the nodes of the network. This models enhanced transport along white matter neural pathways. (iii) Transitions between nodes occur after random, power law distributed, waiting times. This models anomalously slowed diffusion on local scales.

2.1. Reaction Dynamics on Nodes

Let $c(v_i, t)$, $s(v_i, t)$, and $a(v_i, t)$ denote the concentrations of PrP^C, PrP^{Sc}, and PrP^{Agg} respectively at node v_i at time t. The set of ODEs governing the reaction dynamics on a single node is given by

$$\frac{dc(v_i,t)}{dt} = \nu_0 - k_a c(v_i,t) - k_b c(v_i,t)s(v_i,t), \tag{2.1}$$

$$\frac{ds(v_i,t)}{dt} = k_b c(v_i,t)s(v_i,t) - (k_c + k_d)s(v_i,t), \tag{2.2}$$

$$\frac{da(v_i,t)}{dt} = k_c s(v_i,t). \tag{2.3}$$

In these equations; ν_0 parameterises the creation of new PrP^C, k_a and k_d the degradation of PrP^C and PrP^{Sc} respectively, k_b the conversion of PrP^C into PrP^{Sc}, and k_c the conversion of PrP^{Sc} into PrP^{Agg}.

The reduced coupled system of equations, Eq.(2.1) and Eq.(2.2), has a disease free steady state and an endemic steady state. The disease free state is given by

$$c(v_i,t) = \frac{\nu_0}{k_a} \text{ and } s(v_i,t) = 0. \tag{2.4}$$

The endemic steady state is given by

$$c(v_i,t) = \frac{k_c + k_d}{k_b} \text{ and } s(v_i,t) = \frac{k_b\nu_0 - (k_c + k_d)k_a}{(k_c + k_d)k_b}. \tag{2.5}$$

The aggregate, $a(v_i, t)$, remains zero in the disease free state but it grows linearly in time in the endemic steady state.

2.2. Enhanced Transport on a Network

By observing the diffusion of water molecules, Diffusion Tensor Imaging (DTI) [59] is used to identify neural pathways that enhance transport in the brain. These pathways can be represented mathematically by a network of N undirected nodes with edge weights. The edge weights, denoted by $w_{i,j}$ correspond to the number of fibres in a fibre bundle connecting the two nodes v_i and v_j. If there is no edge between v_i and v_j then $w_{i,j} = 0$. The model equations governing transport on a network are then given by

$$\frac{dC(v_i,t)}{dt} = \frac{1}{\tau}\sum_{j=1}^{N}\lambda_{j,i}C(v_j,t) - \frac{1}{\tau}\sum_{j=1}^{N}\lambda_{i,j}C(v_i,t) \tag{2.6}$$

where $C(v_i,t)$ is the number of particles on node v_i at time t, and $\lambda_{i,j}$ are normalized weights defined by

$$\lambda_{i,j} = \frac{w_{i,j}}{\sum_{m=1}^{N} w_{i,m}}. \tag{2.7}$$

The parameter τ has been introduced as a scale factor with the dimensions of time. To obtain an equation in terms of concentration we need to divide by the volume of the node. If node v_i has volume V_i, then the transport equation for the concentration, $c(v_i,t)$, on the network is

$$\frac{dc(v_i,t)}{dt} = \frac{1}{\tau}\sum_{j=1}^{N}\lambda_{j,i}\frac{V_j}{V_i}c(v_j,t) - \frac{1}{\tau}\sum_{j=1}^{N}\lambda_{i,j}c(v_i,t) \tag{2.8}$$

In general it is difficult to obtain the volumes of each node from available experimental data, but it is still possible to infer these volumes from the edge weights. In the long time limit, in the absence of reactions, the concentration on each node must be the same. In order for this limit to hold we let $V_i = \kappa\sum_{j=1}^{N} w_{i,j}$ where κ is a constant with the dimensions of volume. The transport equation can then be written,

$$\frac{dc(v_i,t)}{dt} = \frac{1}{\tau}\sum_{j=1}^{N}\frac{w_{j,i}}{\sum_{m=1}^{N} w_{i,m}}c(v_j,t) - \frac{1}{\tau}\sum_{j=1}^{N}\frac{w_{i,j}}{\sum_{m=1}^{N} w_{i,m}}c(v_i,t). \tag{2.9}$$

As the wights $w_{i,j}$ are symmetric, this can be further simplified to,

$$\frac{dc(v_i,t)}{dt} = \frac{1}{\tau}\sum_{j=1}^{N}\frac{w_{j,i}}{\sum_{m=1}^{N} w_{i,m}}\left(c(v_j,t) - c(v_i,t)\right). \tag{2.10}$$

Considering the case of reactions and transport, applying the reaction dynamics for prion disease introduced above the governing equations are,

$$\begin{aligned}\frac{dc(v_i,t)}{dt} &= \nu_0 - k_a c(v_i,t) - k_b c(v_i,t)s(v_i,t)\\ &\quad + \frac{1}{\tau}\sum_{j=1}^{N}\frac{w_{j,i}}{\sum_{m=1}^{N} w_{i,m}}\left(c(v_j,t) - c(v_i,t)\right),\end{aligned} \tag{2.11}$$

$$\begin{aligned}\frac{ds(v_i,t)}{dt} &= k_b c(v_i,t)s(v_i,t) - (k_c + k_d)s(v_i,t)\\ &\quad + \frac{1}{\tau}\sum_{j=1}^{N}\frac{w_{j,i}}{\sum_{m=1}^{N} w_{i,m}}\left(s(v_j,t) - s(v_i,t)\right),\end{aligned} \tag{2.12}$$

$$\frac{da(v_i,t)}{dt} = k_c s(v_i,t), \tag{2.13}$$

If $\tau \gg 1/k$, where k is the minimum reaction rate, then the transport is very slow compared with the time scale of reactions. For the purposes of this model it is important that the reactions have time to be well mixed before transport occurs.

2.3. Local Anomalous Diffusion

We assume that on local scales, for example the size of voxels in imaging studies, the diffusion of particles is anomalously slowed. This is referred to as subdiffusion if the mean square displacement of diffusing particles scales as a sublinear power law in time, i.e., $\langle x^2 \rangle \sim t^\alpha$, with the scaling exponent $\alpha \in (0, 1)$. It is straightforward to show that the first passage time distribution of subdiffusing particles exiting a voxel is power law distributed with the same scaling exponent. The first passage time results for subdiffusion can readily be obtained from the time subordination of first passage time results in standard diffusion [60].

The solution of the standard diffusion equation with an absorbing boundary can be written as

$$u(x,t) = \sum_{n=0}^{\infty} a_n X_n(x) e^{-p_n^2 Dt}, \tag{2.14}$$

where X_n is the n^{th} eigenfunction of the Laplacian with eigenvalue p_n and the constants c_n can be determined from the initial condition, together with the orthogonality condition of the eigenfunctions. This solution can be used to provide the solution to the subdiffusion problem using time subordination. Under time subordination the temporal term $e^{-p_n^2 Dt}$ is replaced with a heavy tailed Mittag-Leffler function, $E_\alpha(-p_n^2 Dt^\alpha)$, [42] and this results in the subdiffusion solution

$$u_\alpha(x,t) = \sum_{n=0}^{\infty} a_n X_n(x) E_\alpha[-p_n^2 Dt^\alpha], \tag{2.15}$$

where α is the anomalous exponent on the scale of a voxel.

The survival density at time, denoted by $\Phi_\alpha(t)$, is the total of what remains in the local domain, Ω, at t. Formally we write

$$\Phi_\alpha(t) = \int_\Omega u_\alpha(x,t)dx \tag{2.16}$$

$$= \int_\Omega \sum_{n=0}^{\infty} a_n X_n(x) E_\alpha[-p_n^2 Dt]dx. \tag{2.17}$$

The long time behaviour is dominated by the largest non-zero eigenvalue, p_{max}, resulting in the long time scaling

$$\Phi_\alpha(t) \sim E_\alpha[-p_{max}^2 Dt^\alpha] = E_\alpha\left[-\left(\frac{t}{\tau}\right)^\alpha\right] \sim \frac{\tau^\alpha}{\Gamma(1-\alpha)}\frac{1}{t^\alpha}. \tag{2.18}$$

2.4. Network Model with Reactions and Local Anomalous Diffusion

A continuous time random walk model, including reactions on nodes with randomly distributed waiting times before transitions between nodes, was introduced earlier by the authors in [55]. In the model considered here, the waiting times, which arise from locally anomalous diffusion, can be obtained from the survival density in Eq.(2.18). The waiting time density is then given by

$$\psi(t) = -\frac{d\Phi_\alpha(t)}{dt}$$

$$= \left(\frac{t^{\alpha-1}}{\tau^\alpha}\right) E_{\alpha,\alpha}\left[-\left(\frac{t}{\tau}\right)^\alpha\right], \tag{2.19}$$

where

$$E_{a,b}[t] = \sum_{k=0}^{\infty} \frac{t^k}{\Gamma(an+b)} \tag{2.20}$$

is the generalised Mittag-Leffler function [61]. The density in Eq.(2.19) is one of the characteristic heavy tailed waiting time densities employed in CTRW models for subdiffusion. This is a clear demonstration that the anomalous exponent for subdiffusion on the scale of voxels can be carried across to model anomalous transport through a CTRW on a network [55]. In the CTRW model on a network the normalized weights defined in Eq(2.7) become the transition probabilities. The general master equations for a CTRW on a network with Mittag-Leffler waiting time densities and reaction kinetics on the nodes were first derived in [55]. Using the reaction dynamics given by Eqs. (2.1), (2.2), (2.3), in these master equations, we obtain the master equations for the prion model, incorporating local subdiffusion, local reactions and enhanced transport on neural pathways:

$$\begin{aligned}\frac{dc(v_i,t)}{dt} &= \nu_0 - k_a c(v_i,t) - k_b c(v_i,t)s(v_i,t) \\ &\quad + \frac{1}{\tau^\alpha}\sum_{j=1}^{N}\frac{w_{i,j}}{\sum_{m=1}^{N} w_{i,m}}\left(e^{-\int_0^t k_b s(v_j,t')dt' - k_a t}\,{}_0D_t^{1-\alpha}\left[\frac{c(v_j,t)}{e^{-\int_0^t k_b s(v_j,t')dt' - k_a t}}\right]\right. \\ &\quad \left. - e^{-\int_0^t k_b s(v_i,t')dt' - k_a t}\,{}_0D_t^{1-\alpha}\left[\frac{c(v_i,t)}{e^{-\int_0^t k_b s(v_i,t')dt' - k_a t}}\right]\right) \qquad (2.21)\\ \frac{ds(v_i,t)}{dt} &= k_b c(v_i,t)s(v_i,t) - (k_c+k_d)s(v_i,t) \\ &\quad + \frac{1}{\tau^\alpha}\sum_{j=1}^{N}\frac{w_{i,j}}{\sum_{m=1}^{N} w_{i,m}}\left(e^{-(k_c+k_d)t}\,{}_0D_t^{1-\alpha}\left[\frac{s(v_j,t)}{e^{-(k_c+k_d)t}}\right]\right. \\ &\quad \left. - e^{-(k_c+k_d)t}\,{}_0D_t^{1-\alpha}\left[\frac{s(v_i,t)}{e^{-(k_c+k_d)t}}\right]\right) \qquad (2.22)\\ \frac{da(v_i,t)}{dt} &= k_c s(v_i,t). \qquad (2.23)\end{aligned}$$

Here

$${}_0D_t^{1-\alpha}[y(x,t)] = \frac{1}{\Gamma(\alpha)}\frac{d}{dt}\int_0^t \frac{y(x,t')}{(t-t')^{1-\alpha}}\,dt'. \qquad (2.24)$$

is the Riemann-Liouville fractional derivative of order $1-\alpha$, and we have assumed that the fractional integral ${}_0D_t^{-\alpha}[y(x,t)]$ vanishes at $t=0$. In this model the aggregates are stationary and so there is no fractional diffusive component in Eq. (2.23). Note that when $\alpha = 1$, this set of equations recovers the standard set of network reaction transport equations, Eqs.(2.11), (2.12), and (2.13).

3. Model Simulations

In this section we report our results on numerical solutions of the model equations, Eqs.(2.21), (2.22), and (2.23), using an implicit method, described below, and using a brain network obtained from the UCLA Multimodal Connectivity Database [62]. A single 264 node network, named TD32C_DTI in the database, was chosen from the "Typically developing" group of a study into the structural brain networks of individuals with autism [63].

To numerically solve Eqs. (2.21) – (2.23) we use a method similar to the implicit method introduced by Langlands and Henry [58] for solving the fractional subdiffusion equation

$$\frac{\partial u}{\partial t} = D\,{}_0D_t^{1-\alpha}\left(\frac{\partial^2 u}{\partial x^2}\right). \qquad (3.1)$$

Let $t_n = (n-1)\Delta t$ be equally-spaced time points in the interval $t \in [0,T]$ where $\Delta t = T/(M+1)$ is the constant time step, $n = 1,2,3,\ldots,M+1$ and M is the number of time steps. We denote the numerical

approximation for each of the unknowns $c(v_i,t)$, $s(v_i,t)$ and $a(v_i,t)$, at vertex v_i and time t_n, by $c_i^{(n)}$, $s_i^{(n)}$, and $a_i^{(n)}$ respectively. The subscript denotes the vertex and the superscript denotes the time step.

As in [58] we approximate the first order time derivatives on the left of Eqs. (2.21), (2.22), and (2.23) using a backward finite difference at the time t_{n+1} and the right-hand side of these equations are evaluated at the time $t = t_{n+1}$. Eq. (2.23) then becomes

$$\frac{a_i^{(n+1)} - a_i^{(n)}}{\Delta t} = k_c s_i^{(n+1)} \tag{3.2}$$

or

$$a_i^{(n+1)} - k_c \Delta t s_i^{(n+1)} = a_i^{(n)}. \tag{3.3}$$

To evaluate the Riemann-Liouville fractional derivative as in Eqs. (2.21) and (2.22), we use the L1 approximation for the fractional derivative of order $1-\alpha$, with respect to time, of the function $y(t)$ at $t = t_{n+1}$. Using the L1 approximation from [64] we can write this as

$${}_0D_t^{1-\alpha} y(t) \approx \frac{\Delta t^{\alpha-1}}{\Gamma(1+\alpha)} \left\{ \Omega_n(\alpha) y^{(1)} + y^{(n+1)} + \sum_{l=2}^{n} \Theta_{n-l+2}(\alpha) y^{(l)} \right\}, \tag{3.4}$$

where

$$y^{(n)} = y((n-1)\Delta t), \quad n \geq 1, \tag{3.5}$$

$$\Theta_n(\alpha) = n^\alpha - 2(n-1)^\alpha + (n-2)^\alpha, \quad n \geq 2, \tag{3.6}$$

$$\Omega_n(\alpha) = \frac{\alpha}{n^{1-\alpha}} - (n^\alpha - (n-1)^\alpha), \quad n \geq 1, \tag{3.7}$$

and $\Gamma(x)$ is the Gamma function.

Using Eq. (3.4) to approximate the fractional derivative in Eq. (2.22) we find

$$\begin{aligned}
\frac{s_i^{(n+1)} - s_i^{(n)}}{\Delta t} &= k_b c_i^{(n+1)} s_i^{(n+1)} - (k_c + k_d) s_i^{(n+1)} \\
&+ \frac{\Delta t^{\alpha-1}}{\tau^\alpha \Gamma(1+\alpha)} \sum_{j=1}^{N} \frac{w_{i,j}}{\sum_{m=1}^{N} w_{i,m}} \left(\left[\Omega_n(\alpha) s_j^{(1)} e^{-(k_c+k_d)n\Delta t} + s_j^{(n+1)} + \sum_{l=2}^{n} \Theta_{n-l+2}(\alpha) s_j^{(l)} e^{-(k_c+k_d)(n+1-l)\Delta t} \right] \right. \\
&\left. - \left[\Omega_n(\alpha) s_i^{(1)} e^{-(k_c+k_d)n\Delta t} + s_i^{(n+1)} + \sum_{l=2}^{n} \Theta_{n-l+2}(\alpha) s_i^{(l)} e^{-(k_c+k_d)(n+1-l)\Delta t} \right] \right)
\end{aligned} \tag{3.8}$$

which simplifies to

$$\begin{aligned}
s_i^{(n+1)} - k_b c_i^{(n+1)} s_i^{(n+1)} \Delta t + (k_c + k_d) s_i^{(n+1)} \Delta t + \rho \sum_{j=1}^{N} \frac{w_{i,j}}{\sum_{m=1}^{N} w_{i,m}} \left(s_i^{(n+1)} - s_j^{(n+1)} \right) &= s_i^{(n)} \\
+ \rho \sum_{j=1}^{N} \frac{w_{i,j}}{\sum_{m=1}^{N} w_{i,m}} \left(\left[\Omega_n(\alpha) s_j^{(1)} e^{-(k_c+k_d)n\Delta t} + \sum_{l=2}^{n} \Theta_{n-l+2}(\alpha) s_j^{(l)} e^{-(k_c+k_d)(n+1-l)\Delta t} \right] \right. \\
\left. - \left[\Omega_n(\alpha) s_i^{(1)} e^{-(k_c+k_d)n\Delta t} + \sum_{l=2}^{n} \Theta_{n-l+2}(\alpha) s_i^{(l)} e^{-(k_c+k_d)(n+1-l)\Delta t} \right] \right)
\end{aligned} \tag{3.9}$$

where

$$\rho = \frac{\Delta t^\alpha}{\tau^\alpha \Gamma(1+\alpha)}. \tag{3.10}$$

To evaluate the integral of $s(v_i,t)$ in Eq. (2.21) we take advantage that the solution of Eq. (2.23) is

$$a_i(t) = a_i(0) + \int_0^t k_c s_i(t')\,dt' \tag{3.11}$$

and so

$$\int_0^t k_b s_i(t')\,dt' = \frac{k_b}{k_c}\left(a_i(t) - a_i(0)\right) = \beta\left(a_i(t) - a_i(0)\right) \tag{3.12}$$

where $\beta = k_b/k_c$. Now using Eqs. (3.4) and (3.12), Eq. (2.21) is discretized as

$$\begin{aligned}\frac{c_i^{(n+1)} - c_i^{(n)}}{\Delta t} &= \nu_0 - k_a c_i^{(n+1)} - k_b c_i^{(n+1)} s_i^{(n+1)} \\ &+ \frac{\Delta t^{\alpha-1}}{\tau^\alpha \Gamma(1+\alpha)} \sum_{j=1}^{N} \frac{w_{i,j}}{\sum_{m=1}^{N} w_{i,m}} \left(\left[\Omega_n(\alpha) c_j^{(1)} e^{-\beta\left(a_j^{(n+1)} - a_j^{(1)}\right) - k_a n \Delta t} + c_j^{(n+1)} \right.\right. \\ &\left. + \sum_{l=2}^{n} \Theta_{n-l+2}(\alpha) c_j^{(l)} e^{-\beta\left(a_j^{(n+1)} - a_j^{(l)}\right) - k_a (n+1-l)\Delta t} \right] \\ &\left. - \left[\Omega_n(\alpha) c_i^{(1)} e^{-\beta\left(a_i^{(n+1)} - a_i^{(1)}\right) - k_a n \Delta t} + c_i^{(n+1)} + \sum_{l=2}^{n} \Theta_{n-l+2}(\alpha) c_i^{(l)} e^{-\beta\left(a_i^{(n+1)} - a_i^{(l)}\right) - k_a (n+1-l)\Delta t} \right] \right)\end{aligned} \tag{3.13}$$

or

$$\begin{aligned}c_i^{(n+1)} + k_a c_i^{(n+1)} \Delta t + k_b c_i^{(n+1)} s_i^{(n+1)} \Delta t + \rho \sum_{j=1}^{N} \frac{w_{i,j}}{\sum_{m=1}^{N} w_{i,m}} \left(c_i^{(n+1)} - c_j^{(n+1)} \right) \\ = c_i^{(n)} + \nu_0 \Delta t + \rho \sum_{j=1}^{N} \frac{w_{i,j}}{\sum_{m=1}^{N} w_{i,m}} \left(\left[\Omega_n(\alpha) c_j^{(1)} e^{-\beta\left(a_j^{(n+1)} - a_j^{(1)}\right) - k_a n \Delta t} \right.\right. \\ \left. + \sum_{l=2}^{n} \Theta_{n-l+2}(\alpha) c_j^{(l)} e^{-\beta\left(a_j^{(n+1)} - a_j^{(l)}\right) - k_a (n+1-l)\Delta t} \right] \\ \left. - \left[\Omega_n(\alpha) c_i^{(1)} e^{-\beta\left(a_i^{(n+1)} - a_i^{(1)}\right) - k_a n \Delta t} + \sum_{l=2}^{n} \Theta_{n-l+2}(\alpha) c_i^{(l)} e^{-\beta\left(a_i^{(n+1)} - a_i^{(l)}\right) - k_a (n+1-l)\Delta t} \right] \right).\end{aligned} \tag{3.14}$$

Eqs. (3.3), (3.9) and (3.14) form a system of nonlinear equations which is solved using the Newton-Raphson procedure.

Initial conditions were chosen as follows; $c(v_i,0) = 1$, $s(v_i,0) = 0$ and $a(v_i,0) = 0$ for all nodes except at six seed nodes where $s(v_i,0) = 0.01$ and $c(v_i,0) = 0.99$. These conditions ensure that initially there is the same total number of PrP^C and PrP^{Sc} at each node, i.e. $s(v_i,0) + c(v_i,0) = 1$. The seeded nodes correspond to the inferior temporal cortex region of the brain. The formation of aggregates in these regions of the brain have been observed in very early cases of Alzheimer's Disease [17].

It is difficult to provide reliable estimates for model parameters. The parameters used in our simulations are chosen to show the effects of changing the subdiffusive exponent α. The rate parameters, in arbitrary units, were taken to be $\nu_0 = 60$, $k_a = 60$, $k_b = 60$, $k_c = 30$ and $k_d = 20$. The time scale parameter was set at $\tau = 1$.

Figure 1 shows plots of the concentrations of proteins and aggregates, taken over all nodes, as a function of time for three different values of α. On each node the concentration of PrP^{C} and PrP^{Sc} tends towards their endemic steady state values, Eq.(2.5). The concentration of the aggregate PrP^{Agg} tends towards a linear increase in time at the same rate across all nodes. It is clear from this figure that as α is decreased (more anomalous) the system approaches the equilibrium state faster with less variation in the concentrations of proteins and aggregates across the network. The profile of concentration versus time is similar for all nodes. On each node the disease free steady state is destablilized by the arrival of PrP^{Sc} whose concentration then increases to the endemic steady state. This behaviour is typical of a propagating front. The propagation can be seen in plots of the spatial spread of the disease.

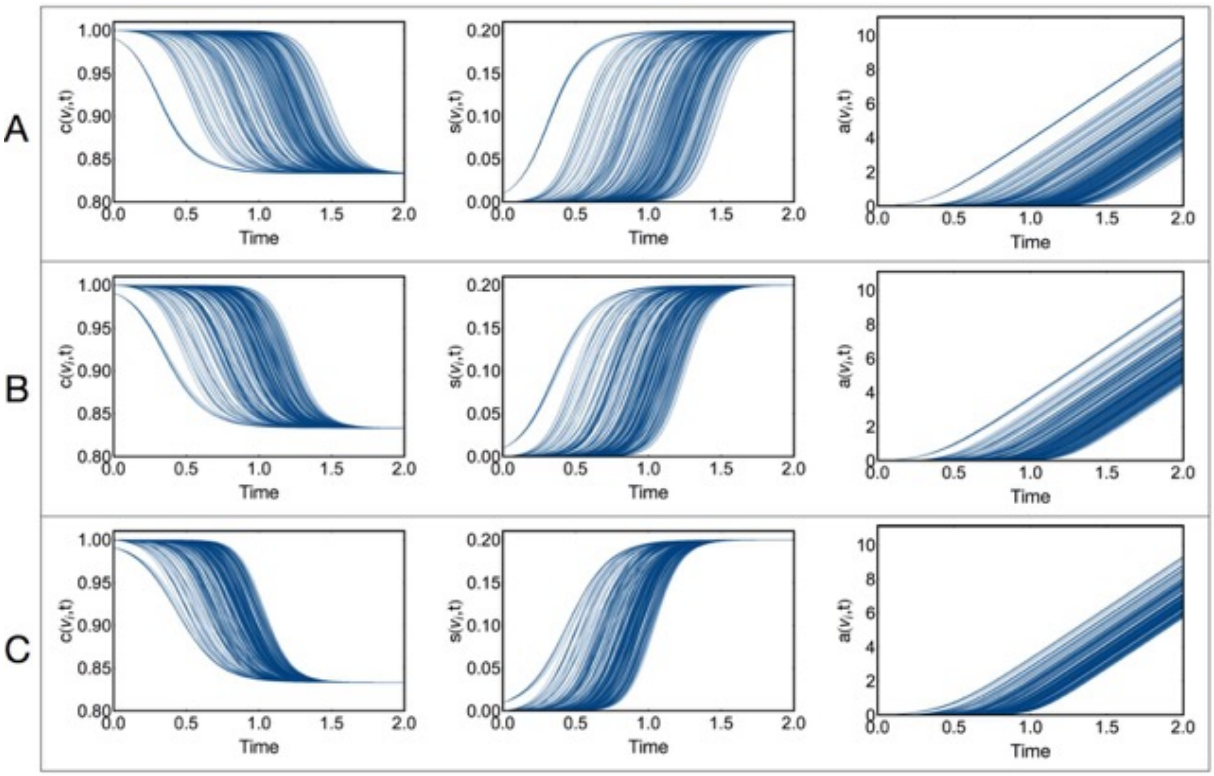

FIGURE 1. Node concentration of PrP^{C} (*Left*), PrP^{Sc} (*Centre*) and PrP^{Agg} (*Right*) up till time $t = 2$: (**A**), $\alpha = 1$; (**B**), $\alpha = 0.8$; (**C**), $\alpha = 0.6$.

Figures 2, 3, 4 show the spatial spread of the concentrations of the diseased protein, PrP^{Sc}, across an XY projection of the brain network for $\alpha = 0.6$, $\alpha = 0.8$, and $\alpha = 1.0$, respectively. At $\alpha = 0.6$ all nodes appear to have reached the equilibrium concentration for diseased proteins by time $t = 1.4$. For $\alpha = 0.8$ more than half of the nodes, but not all, have reached the equilibrium concentration levels by this time whereas for $\alpha = 1.0$ less than half of the nodes have reached the equilibrium concentration levels. From these figures is can be seen that the concentration of diseased proteins builds up faster on nodes at the rear of the brain. This is due to the initial conditions and the network topology. Taken together the plots in Figures 1-4 provide evidence that this spread can be described as a propagating front with the endemic disease state moving from the seeded parts of the brain to the other parts of the brain at different times. The front appears to move faster for lower values of α. This can be explained by the early time behaviour of the waiting time survival function. At early times, the Mittag-Leffler survival function is larger for

values of α closer to one, hence for small α a larger proportion of particles will jump at early times. The destabilization of the disease free state only requires a low concentration of particles. As such the long time trapping of even the majority of particles is insufficient to prevent the propagation of the disease.

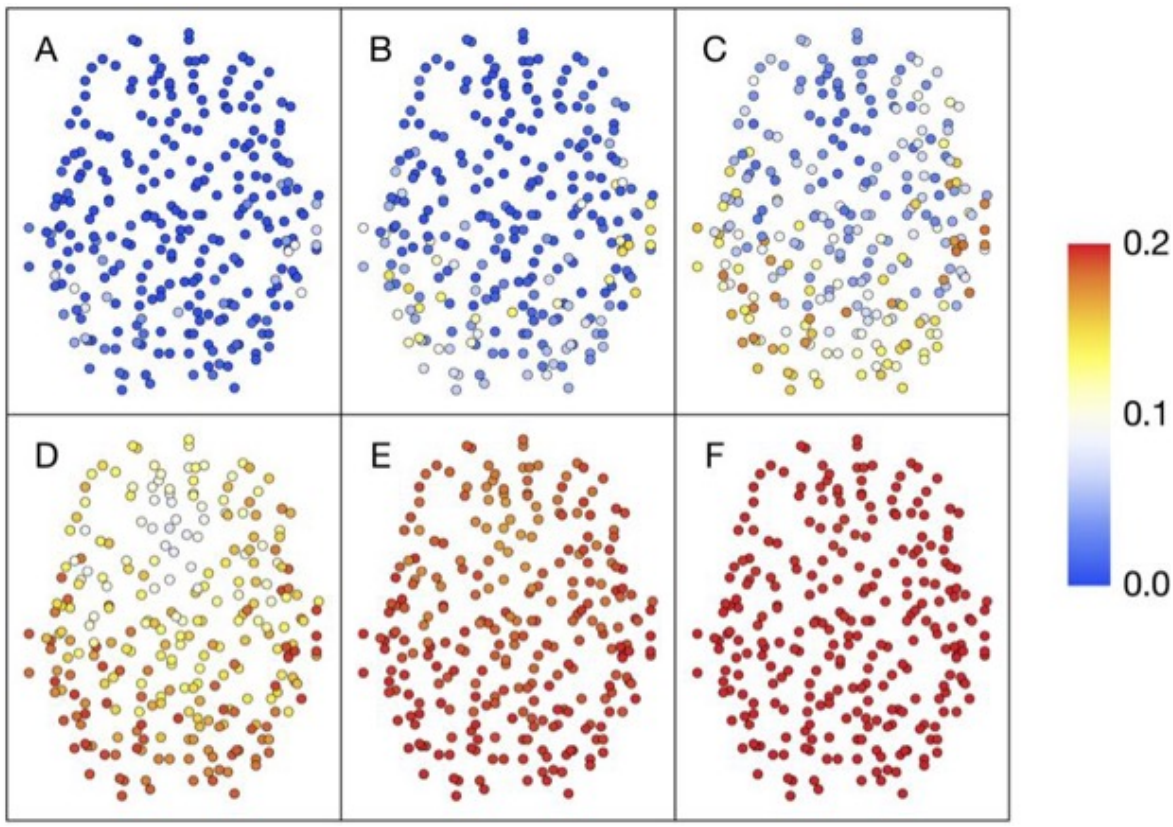

FIGURE 2. The concentration of PrP^{Sc} across the network at times, $t = 0.4$ (A), $t = 0.6$ (B), $t = 0.8$ (C), $t = 1.0$ (D), $t = 1.2$ (E), and $t = 1.4$ (F) with $\alpha = 0.6$.

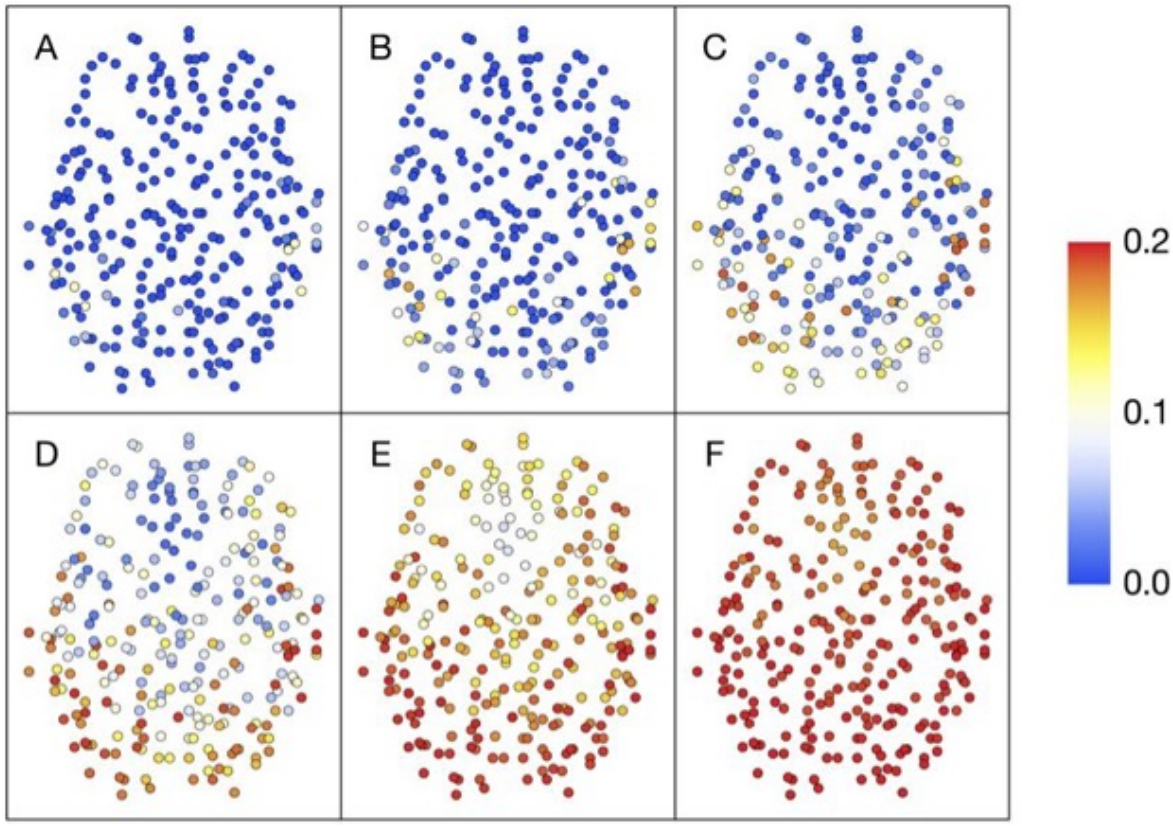

FIGURE 3. The concentration of PrP^{Sc} across the network at times, $t = 0.4$ (A), $t = 0.6$ (B), $t = 0.8$ (C), $t = 1.0$ (D), $t = 1.2$ (E), and $t = 1.4$ $(F)$with $\alpha = 0.8$.

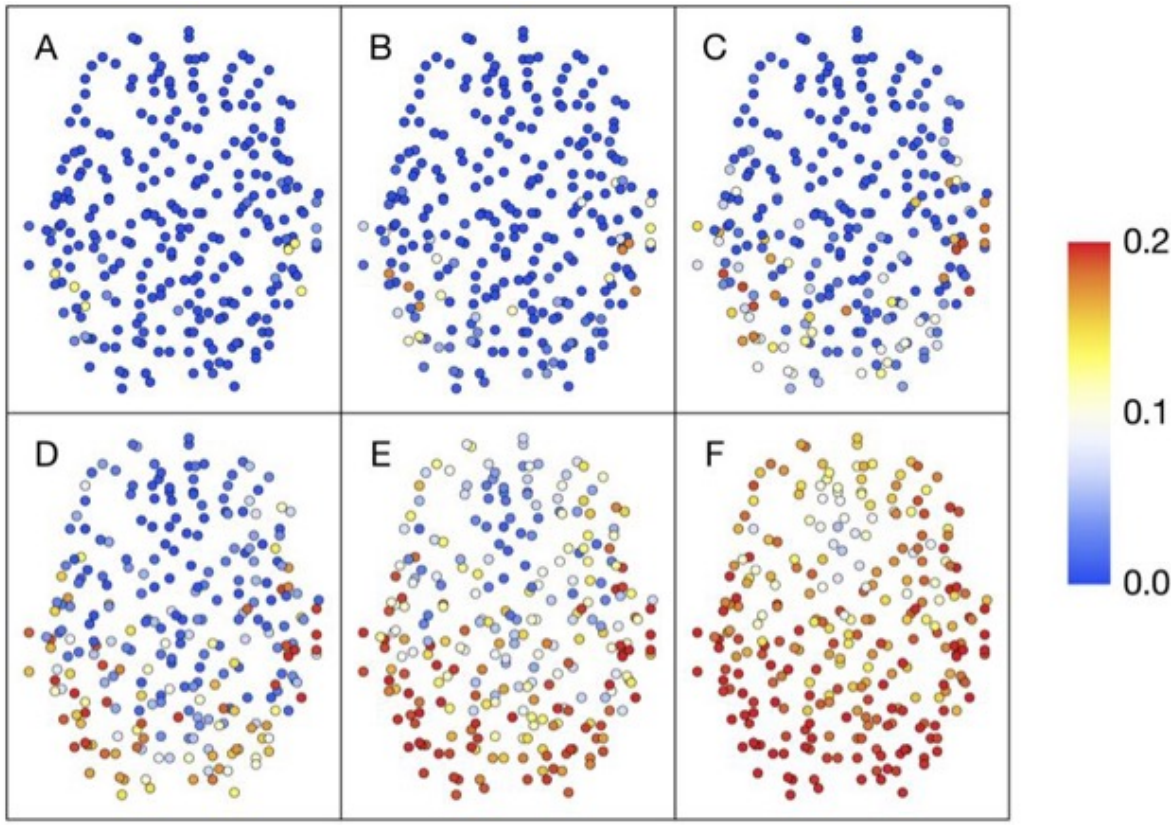

FIGURE 4. The concentration of PrP^{Sc} across the network at times, $t = 0.4$ (A), $t = 0.6$ (B), $t = 0.8$ (C), $t = 1.0$ (D), $t = 1.2$ (E), and $t = 1.4$ $(F)$with $\alpha = 1.0$.

4. Discussion

The movements of particles, including disease particles, in the brain and the resultant disease progression in the brain is confounded by microscopic trapping and binding of particles on the one hand and the relatively free movements of particles along neural pathways on the other. We have introduced a model that can incorporate both these transport features along with reaction dynamics modelling disease processes. The neural pathways are routinely obtained from diffusion tensor imaging and represented as networks with edge weights quantifying the number of fibres, and hence ease of transport, between nodes. Our mathematical model is a network model with transport between nodes and reactions on nodes. The microscopic trapping of particles motivates the introduction of a heavy tailed waiting time density in a continuous time random walk on the network, with jump probabilities defined by normalized edge weights. The reaction dynamics are then incorporated into this model using the formalism derived in [55].

Modelling the spatial progression of prion and prionoid diseases is fundamental to the understanding and treatment of these diseases and we hope that the model developed here could be a useful starting point for further studies. In the simulations presented here, there is evidence that subdiffusion on local scales could impact on disease progression across large scales but there are two problems with the model as it stands. One problem, which is ubiquitous in brain network models, is the choice of model parameters. A second problem, which is fundamental to models for the spatial spread of disease on brain networks, is that transport between the nodes on the network is instantaneous whereas the physical transport in the

brain between such points is very complex and certainly not instantaneous. The prevalence of anomalous diffusion in the brain and the increasing availability of brain network models makes this an important area for future work.

Acknowledgements. This work was supported by the Australian Commonwealth Government (ARC DP140101193).

References

[1] M. Jucker, L. C. Walker, *Pathogenic protein seeding in Alzheimer disease and other neurodegenerative disorders,*Ann Neurol, vol. 70, no. 4, pp. 532–540, 2011.

[2] S. B. Prusiner, *Novel proteinaceous infectious particles cause scrapie,* Science, vol. 216, no. 4542, pp. 136–144, 1982.

[3] ——, *Prion biology and diseases.* Cold Spring Harbor Laboratory Press, 2004.

[4] K. Brown, J. A. Mastrianni, *The prion diseases,* J. Geriatr. Psychiatry Neurol., vol. 23, no. 4, pp. 277–298, 2010.

[5] A. Aguzzi, L. Rajendran, *The transcellular spread of cytosolic amyloids, prions, and prionoids,* Neuron, vol. 64, no. 6, pp. 783–790, 2009.

[6] M. Cushman, B. S. Johnson, O. D. King, A. D. Gitler, J. Shorter, *Prion-like disorders: blurring the divide between transmissibility and infectivity,* J. Cell Sci., vol. 123, no. 8, pp. 1191–1201, 2010.

[7] C. Duyckaerts, B. Delatour, M.-C. Potier, *Classification and basic pathology of Alzheimer disease,* Acta Neuropathol., vol. 118, no. 1, pp. 5–36, 2009.

[8] H. Braak, K. Del Tredici, *Nervous system pathology in sporadic Parkinson disease,* Neurol., vol. 70, no. 20, pp. 1916–1925, 2008.

[9] L. C. Walker, H. LeVine, *Corruption and spread of pathogenic proteins in neurodegenerative diseases,* J. Bio. Chem., vol. 287, no. 40, pp. 33 109–33 115, 2012.

[10] M. Jucker and L. C. Walker, *Self-propagation of pathogenic protein aggregates in neurodegenerative diseases,* Nature, vol. 501, no. 7465, pp. 45–51, 2013.

[11] H. Baker, R. Ridley, L. Duchen, T. Crow, C. Bruton, *Evidence for the experimental transmission of cerebral beta-amyloidosis to primates.* Int. J Exp. Pathol., vol. 74, no. 5, p. 441, 1993.

[12] R. Ridley, H. Baker, C. Windle, R. Cummings, *Very long term studies of the seeding of β-amyloidosis in primates,* J Neural Transm., vol. 113, no. 9, pp. 1243–1251, 2006.

[13] J. Goudsmit, C. H. Morrow, D. M. Asher, R. T. Yanagihara, C. L. Masters, C. J. Gibbs, D. C. Gajdusek, *Evidence for and against the transmissibility of Alzheimer disease,* Neurology, vol. 30, no. 9, pp. 945–945, 1980.

[14] S. B. Prusiner, *Prions,* Proc. Nat. Aca. Sci., vol. 95, no. 23, pp. 13 363–13 383, 1998.

[15] S.-J. Lee, P. Desplats, C. Sigurdson, I. Tsigelny, E. Masliah, *Cell-to-cell transmission of non-prion protein aggregates,* Nature Reviews Neurology, vol. 6, no. 12, pp. 702–706, 2010.

[16] C. Saper, B. Wainer, D. German, *Axonal and transneuronal transport in the transmission of neurological disease: potential role in system degenerations, including Alzheimer's disease,* Neuroscience, vol. 23, no. 2, pp. 389–398, 1987.

[17] H. Braak, E. Braak, *Neuropathological stageing of Alzheimer-related changes, Acta Neuropathol.*, vol. 82, no. 4, pp. 239–259, 1991.

[18] D. R. Thal, U. Rüb, M. Orantes, and H. Braak, *Phases of Aβ-deposition in the human brain and its relevance for the development of ad,* Neurology, vol. 58, no. 12, pp. 1791–1800, 2002.

[19] H. Braak, K. Del Tredici, U. Rüb, R. A. de Vos, E. N. J. Steur, E. Braak, *Staging of brain pathology related to sporadic Parkinson?s disease,* Neurobiology of aging, vol. 24, no. 2, pp. 197–211, 2003.

[20] J. M. Ravits and A. R. La Spada, *ALS motor phenotype heterogeneity, focality, and spread deconstructing motor neuron degeneration,* Neurology, vol. 73, no. 10, pp. 805–811, 2009.

[21] J. Brettschneider, K. Del Tredici, J. B. Toledo, J. L. Robinson, D. J. Irwin, M. Grossman, E. Suh, V. M. Deerlin, E. M. Wood, Y. Baek et al., *Stages of pTDP-43 pathology in amyotrophic lateral sclerosis,* Annals of neurology, vol. 74, no. 1, pp. 20–38, 2013.

[22] M. Goedert, M. G. Spillantini, K. Del Tredici, H. Braak, *100 years of Lewy pathology,* Nature Reviews Neurology, vol. 9, no. 1, pp. 13–24, 2013.

[23] J. Liu, L. Zhao, J. Nan, G. Li, S. Xiong, K. M. von Deneen, Q. Gong, F. Liang, W. Qin, J. Tian, *The trade-off between wiring cost and network topology in white matter structural networks in health and migraine,* Experimental neurology, vol. 248, pp. 196–204, 2013.

[24] D. Le Bihan, J. F. Mangin, C. Poupon, C. Clark, S. Pappata, N. Molko, H. Chabriat, *Diffusion tensor imaging: concepts and applications,* J. Magn. Reson. Im., vol. 13, no. 4, pp. 534–546, 2001.

[25] A. Raj, A. Kuceyeski, M. Weiner, *A network diffusion model of disease progression in dementia,* Neuron, vol. 73, no. 6, pp. 1204 – 1215, 2012.

[26] E. Syková, C. Nicholson, *Diffusion in brain extracellular space,* Physio. Rev., vol. 88, no. 4, pp. 1277–1340, 2008.

[27] E. Özarslan, P. J. Basser, T. M. Shepherd, P. E. Thelwall, B. C. Vemuri, S. J. Blackband, *Observation of anomalous diffusion in excised tissue by characterizing the diffusion-time dependence of the MR signal,* J. Magnet. Reson., vol. 183, no. 2, pp. 315–323, 2006.

[28] E. Özarslan, T. M. Shepherd, C. G. Koay, S. J. Blackband, P. J. Basser, *Temporal scaling characteristics of diffusion as a new MRI contrast: findings in rat hippocampus,* Neuroimage, vol. 60, no. 2, pp. 1380–1393, 2012.

[29] D. Le Bihan, E. Breton, D. Lallemand, P. Grenier, E. Cabanis, M. Laval-Jeantet et al., *MR imaging of intravoxel incoherent motions: application to diffusion and perfusion in neurologic disorders,* Radiology, vol. 161, no. 2, pp. 401–407, 1986.

[30] R. Sener, *Diffusion MRI: apparent diffusion coefficient (ADC) values in the normal brain and a classification of brain disorders based on ADC values,* Comput. Med. Imag. Grap., vol. 25, no. 4, pp. 299–326, 2001.

[31] R. V. Mulkern, H. Gudbjartsson, C.-F. Westin, H. P. Zengingonul, W. Gartner, C. R. Guttmann, R. L. Robertson, W. Kyriakos, R. Schwartz, D. Holtzman et al., *Multi-component apparent diffusion coefficients in human brain,* NMR Biomed., vol. 12, pp. 51–62, 1999.

[32] K. M. Bennett, K. M. Schmainda, D. B. Rowe, H. Lu, J. S. Hyde et al., *Characterization of continuously distributed cortical water diffusion rates with a stretched-exponential model,* Magnet. Reson. Med., vol. 50, no. 4, pp. 727–734, 2003.

[33] M. G. Hall, T. R. Barrick, *From diffusion-weighted MRI to anomalous diffusion imaging,* Magnet. Reson. Med., vol. 59, no. 3, pp. 447–455, 2008.

[34] S. De Santis, A. Gabrielli, M. Bozzali, B. Maraviglia, E. Macaluso, S. Capuani, *Anisotropic anomalous diffusion assessed in the human brain by scalar invariant indices,* Magnet. Reson. Med., vol. 65, no. 4, pp. 1043–1052, 2011.

[35] M. G. Hall, T. R. Barrick, *Two-step anomalous diffusion tensor imaging, NMR in Biomed.*, vol. 25, no. 2, pp. 286–294, 2012.

[36] J. H. Jensen, J. A. Helpern, *MRI quantification of non-Gaussian water diffusion by kurtosis analysis,* NMR in Biomed., vol. 23, no. 7, pp. 698–710, 2010.

[37] R. L. Magin, O. Abdullah, D. Baleanu, X. J. Zhou, *Anomalous diffusion expressed through fractional order differential operators in the Bloch–Torrey equation,* J. Magnet. Reson., vol. 190, no. 2, pp. 255–270, 2008.

[38] X. J. Zhou, Q. Gao, O. Abdullah, R. L. Magin, *Studies of anomalous diffusion in the human brain using fractional order calculus,* Magnet. Reson. Med., vol. 63, no. 3, pp. 562–569, 2010.

[39] B. Fevrier, D. Vilette, F. Archer, D. Loew, W. Faigle, M. Vidal, H. Laude, G. Raposo, *Cells release prions in association with exosomes,* P. Natl. Acad. Sci. USA, vol. 101, no. 26, pp. 9683–9688, 2004.

[40] A. C. Magalhães, G. S. Baron, K. S. Lee, O. Steele-Mortimer, D. Dorward, M. A. Prado, B. Caughey, *Uptake and neuritic transport of scrapie prion protein coincident with infection of neuronal cells,* J. Neurosci., vol. 25, no. 21, pp. 5207–5216, 2005.

[41] R. Hilfer, L. Anton, *Fractional master equations and fractal time random walks,* Phys. Rev. E, vol. 51, p. R848, 1995.

[42] R. Metzler, J. Klafter, *The random walk's guide to anomalous diffusion: a fractional dynamics approach, Phys. Rep.*, vol. 339, no. 1, pp. 1–77, 2000.

[43] E. Barkai, R. Metzler, J. Klafter, *From continuous time random walks to the fractional Fokker-Planck equation,* Phys. Rev. E, vol. 61, no. 1, p. 132, 2000.

[44] I. M. Sokolov, J. Klafter, *Field-induced dispersion in subdiffusion,* Physical review letters, vol. 97, no. 14, p. 140602, 2006.

[45] B. I. Henry, T. A. M. Langlands, P. Straka, *Fractional Fokker-Planck equations for subdiffusion with space- and time-dependent forces,* Phys. Rev. Lett., vol. 105, no. 17, p. 170602, 2010.

[46] B. I. Henry, T. A. M. Langlands, S. L. Wearne, *Anomalous diffusion with linear reaction dynamics: From continuous time random walks to fractional reaction-diffusion equations,* Phys. Rev. E, vol. 74, no. 3, p. 031116, 2006.

[47] S. Fedotov, *Non-Markovian random walks and nonlinear reactions: subdiffusion and propagating fronts,* Physical Review E, vol. 81, no. 1, p. 011117, 2010.

[48] C. N. Angstmann, I. C. Donnelly, B. I. Henry, *Continuous time random walks with reactions, forcing and trapping,* Math. Model. Nat. Phenom., vol. 8, pp. 17–27, 2013.

[49] A. A. Nepomnyashchy, V. A. Volpert, *An exactly solvable model of subdiffusion–reaction front propagation,* Journal of Physics A: Mathematical and Theoretical, vol. 46, no. 6, p. 065101, 2013.

[50] V. A. Volpert, Y. Kanevsky, A. A. Nepomnyashchy, *Propagation failure for a front between stable states in a system with subdiffusion,* Phys. Rev. E, vol. 89, p. 012901, 2014.

[51] B. Henry, T. Langlands, S. Wearne, *Fractional cable models for spiny neuronal dendrites,* Physical review letters, vol. 100, no. 12, p. 128103, 2008.

[52] T. A. M. Langlands, B. I. Henry, S. L. Wearne, *Fractional cable equation models for anomalous electrodiffusion in nerve cells: infinite domain solutions,* Journal of mathematical biology, vol. 59, no. 6, pp. 761–808, 2009.

[53] T. Langlands, B. Henry, S. L. Wearne, *Fractional cable equation models for anomalous electrodiffusion in nerve cells: finite domain solutions,* SIAM Journal on Applied Mathematics, vol. 71, no. 4, pp. 1168–1203, 2011.

[54] C. Ingo, R. L. Magin, L. Colon-Perez, W. Triplett, T. H. Mareci, *On random walks and entropy in diffusion-weighted magnetic resonance imaging studies of neural tissue,* Magnet. Reson. Med., vol. 71, no. 2, pp. 617–627, 2014.

[55] C. N. Angstmann, I. C. Donnelly, B. I. Henry, *Pattern formation on networks with reactions: A continuous-time random-walk approach,* Phys. Rev. E, vol. 87, p. 032804, 2013.

[56] C. N. Angstmann, I. C. Donnelly, B. I. Henry, T. A. M. Langlands, *Continuous-time random walks on networks with vertex- and time-dependent forcing,* Phys. Rev. E, vol. 88, p. 022811, 2013.

[57] F. E. Cohen, K.-M. Pan, Z. Huang, M. Baldwin, R. J. Fletterick, S. B. Prusiner, *Structural clues to prion replication,* Science (New York, NY), vol. 264, no. 5158, p. 530, 1994.

[58] T. A. M. Langlands, B. I. Henry, *The accuracy and stability of an implicit solution method for the fractional diffusion equation,* J Comp. Phys., vol. 205, no. 2, pp. 719 – 736, 2005.

[59] A. L. Alexander, J. E. Lee, M. Lazar, A. S. Field, *Diffusion tensor imaging of the brain,* Neurotherapeutics, vol. 4, no. 3, pp. 316–329, 2007.

[60] A. Erickson, B. Henry, P. Klaase, C. Angstmann, *Predicting first traversal times for virions and nanoparticles in mucus with slowed diffusion,* Biophysical Journal, vol. 109, pp. 164–172, 2015.

[61] H. J. Haubold, A. M. Mathai, R. K. Saxena, *Mittag-leffler functions and their applications,* Journal of Applied Mathematics, vol. 2011, 2011.

[62] J. A. Brown, J. D. Rudie, A. Bandrowski, J. D. Van Horn, S. Y. Bookheimer, *The UCLA Multimodal Connectivity Database: A web-based platform for brain connectivity matrix sharing and analysis,* Frontiers in Neuroinformatics, vol. 6, no. 28, 2012.

[63] J. D. Rudie, J. Brown, D. Beck-Pancer, L. Hernandez, E. Dennis, P. Thompson, S. Bookheimer, M. Dapretto, *Altered functional and structural brain network organization in autism,* NeuroImage: Clinical, vol. 2, pp. 79–94, 2013.

[64] K. B. Oldham and J. Spanier, *The Fractional Calculus:Theory and Applications of Differentiation and Integration to Arbitrary Order.* Academic Press, 1974.